Effects of synchronized inhibition on post-synaptic targets

Stephani Otte

BGGN 260

Abstract

Activated neuronal groups engage in rhythmic synchronization in the gamma- frequency range (30-80Hz). Changes in the level of gamma synchronization are seen in the cortex during a variety of cognitive tasks including working memory maintenance (Pesaran et al., 2002), attentional selection (Fries et al., 2001), and perceptual awareness. Several computational and experimental studies investigating the mechanisms underlying gamma-band synchronization, found that fast-spiking (FS) inhibitory neurons play a prominent role in the generation of this activity. Networks of FS cells synchronize their firing, and impose synchronized inhibition onto subgroups pyramidal neurons effectively controlling their spike probability and timing. Therefore, the level of synchronization of the FS cells could be an important way of regulating the flow of cortical information. Here, I determined how changes in the synchronization of the FS neurons affect the responsiveness of pyramidal neurons, by modeling and simulating changes in inhibitory synchrony. Increases in the synchronization of inhibitory neurons, can increase the spike rate of pyramidal neurons, even though the mean level of inhibition is increasing. These and future studies may lead to a better understanding of how neuronal gamma-band synchronization subserves various cognitive functions.

Introduction

The encoding of information in cortical networks depends on both the rate of action potential generation by individual cells as well as the precise timing of action potential discharge. Fast spiking (FS) inhibitory interneurons innervate the soma, proximal dendrites and axon initial segments of pyramidal neurons, which are anatomically preferred locations for controlling the probability and timing of action potentials. Several modeling and experimental studies, have shown that local networks of FS cells can generate synchronous oscillatiory activity at gamma frequencies (30-80Hz) (Whittington et al., 1995, Jeffrys 1996, Bartos et al., 2007). Therefore, the local networks of FS cells impose rhythmic synchronized inhibitory input onto subgroups of pyramidal neurons, modulating their discharges (Hasenstaub et al., 2005).

There is evidence that the synchronization of the FS networks is a dynamic process. For instance, The Reynolds lab found that when attention is directed to a stimulus within the receptive field of a cortical neuron, narrow spiking cells, putative FS neurons, show a pronounced attention-dependent increase in gamma frequency synchronization (unpublished data from the John Reynolds lab). Changes in gamma-band synchronization have been seen during a variety of other cognitive tasks, such as working memory maintenance (Pesaran et al 2002), sensory stimulation (Gray et al, 1989), sensory-motor-integration, etc. Flexible and dynamic synchronized inhibition would modulate the discharge of the post-synaptic targets, and thus modulate the flow of cortical information in space and time.

I am particularly interested on understanding the physiological and functional consequences of changes in inhibitory synchronization. To determine how changes in the synchronization of the FS neurons affect the responsiveness of pyramidal neurons, I used two approaches modeling and simulating changes in the mean level and temporal structure of the inhibitory input. .

Methods

Modeling: A single-compartment model was implemented in Matlab (Mathworks, Natick, MA). The model contained a leak conductance of 10nS which reversed at -70mV. The model also contained a transient Na+ current and a Kv1-like delayed rectifier K+ current, which were modeling using a Hodgkin-Huxley-type formalism (after Erisir et al, J Neurophys 82:2476, 1999) Forward and reverse rate constants a and b were given by the equations found , and infinite-time open fractions and time constants were calculated according to

$$n_\infty = \frac{\alpha}{\alpha + \beta} \quad \text{and} \quad \tau = \frac{1}{\alpha + \beta}$$

The maximum sodium and potassium conductances were 700 and 1400ns respectively, and the corresponding currents reversed at 50 and -80 mV respectively. A constant level of excitatory current was injected into the model. The inhibitory current was injected as a 40Hz sine wave. The mean level and sine wave amplitude were adjusted, and parameter sweeps were preformed.

Slice preparation/ Intracellular Recordings:
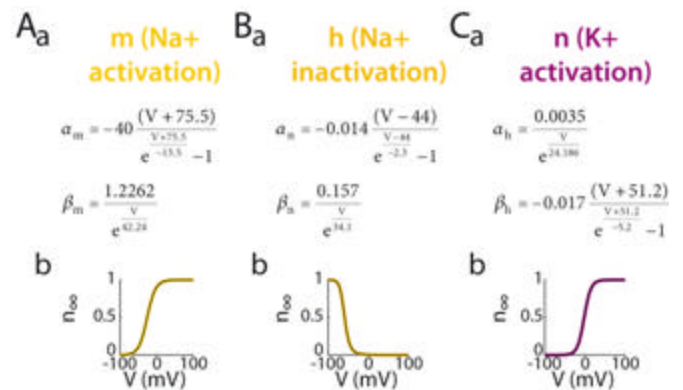
C57/B6 mice, aged P16-P26, were anesthetized with nembutal (100mg/kg i.p.) and decapitated. A vibratome was used to cut 300 um thick coronal brain slices. Slices were cut in ice-cold artificial cerebral spinal fluid (ACSF; 24mM NaCl, 5mM KCl, 26mM NaHCO3, 1mM KH2PO4, 1mM MgSO4, 10mM glucose, 1.2mM CaCl2, and 1mM Kynurenic Acid) and incubated at 35 degrees C for at least 30 minutes in ACSF bubbled with 95% O2/ 5% CO2 before transferring to a room-temperature submerged chamber for recording. Intracellular whole-cell recordings were obtained with glass pipettes pulled on a P-97 micropipette puller (Sutter Instruments, Novato, CA) from borosilicate glass (Sutter Instruments) to 3- 5MOhm, and filled with 130mM D-Gluconate acid, 0.2mM EGTA, 2mM MgCl2 * 6H2O, 6mM KCl, 10mM HEPES, 2.5mM Na-ATP, 0.5mM Na-GTP, and 10mM K-Phophocreatine (pH 7.2). Signals were amplified with an Axopatch-200B or MultiClamp 700B amplifier (Molecular Devices). Data was digitized and collected at 40 KHz using the Spike2 Power1401 collection system (Cambridge Electronic Designs, Cambridge, UK).

Dynamic Clamp:
Fast real-time dynamic clamp was implemented using RTLDC (Boston University) combined with the Re a-time application Interface (www.rtai.org), device drivers from the COMEDI project (www.comedi.org) and a NI board (National Instruments). To minimize the dynamic clamp cycle duration the dynamic clamp computer performed no other tasks and was not used for data acquisition. Series resistance was monitored and compensated periodically throughout the experiment. The dynamic clamp was used to generate excitatory conductance with a reversal potential of 0mV, and inhibitory conductance with a reversal potential of -80mV. The inhibitory conductance was injected as a 40 Hz. sine wave. Parameter sweeps were preformed where the mean level of inhibition and the amplitude of the sine wave varied.

Results

The level and temporal structure of the inhibitory input modulates the spike rate.
The dynamic clamp was used to simulate of a tonic level of excitatory conductance in a pyramidal neuron. Inhibitory conductance was injected as a sine wave, the mean level and temporal structure of the inhibitory conductance was varied. To simulate changes in the synchrony of inhibitory input, the amplitude of the sine wave was varied; increasing the amplitude corresponds to increasing synchrony of the inhibitory inputs. (Figure 1A). The pyramidal neuron's spike rate is plotted as a function of the mean level and the amplitude of the sine wave (Figure 1B).

Figure 1: Level and temporal structure of inhibitory input modulates spike rate.

A. Example recordings from a pyramidal neuron (bottom). Using dynamic clamp a tonic level of excitatory conductance was injected into the neuron (middle). Inhibitory conductance was injected as a sine wave, the mean level and sine wave amplitude were varied (top). **B.** The number of spikes in a 250ms pulse is plotted against the mean level of inhibition (y-axis) and amplitude of the sine wave (x-axis).
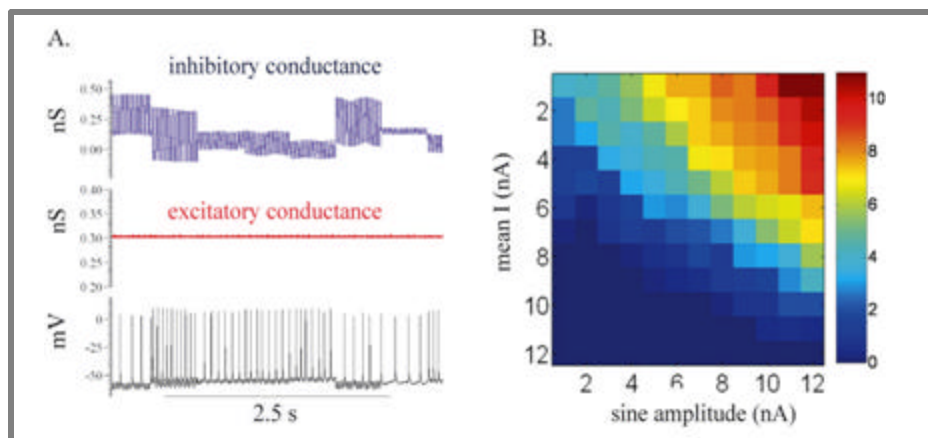
Cells show different dependence of inhibitory input

I recorded from 10 pyramidal neurons in layer 5 of the visual cortex. The neurons that I recorded from showed one of two profiles. Six neuron's spike rate increased as the sine amplitude increased (Figure 2A). Four of the neuron's spike rate did not change as the sine wave amplitude was varied. (Figure 2B) This indicates that the neurons respond differently to changes in the level of inhibitory synchrony.

Figure 2: Cells show different dependence on inhibitory input.

The number of spikes in a 250ms pulse is plotted against the mean level of inhibition and amplitude of the sine wave (Ab+Bb). The same information is also shown as the number of spikes plotted as a function of the amplitude of the sine wave (Aa + Ba) or the mean level of inhibition (Ac+ Bc). Increasing the amplitude of the sine wave increases (Aa) or has no effect (Ba) on the spike count.
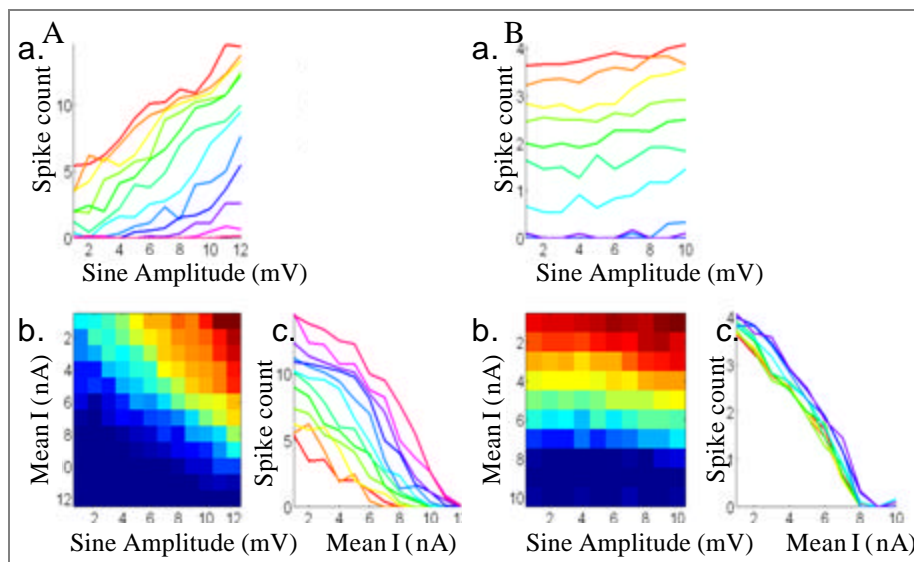
The afterhyperpolarization conductance is important regulator of spike rate.

I used a Hodgkin-Huxley model of a neuron to determine which conductances the neuron has to have to exhibit a profile similar to the cell shown in Figure 2A. A neuron model with only sodium, potassium, and leak conductances did not exhibit a profile that is similar to any of the pyramidal neuron's I recorded from (Figure 3A). When comparing the voltage traces of the model and the real cell, it is obvious that the real cell has a much longer afterhyperpolarization (AHP). (Figure 3B+D) This slow AHP in the real cell is most likely due to calcium activated K+ channels. I therefore added AHP conductance to the model cell. The AHP conductance was modeled as an exponential with a reversal potential of -80mV, a time constant of 40ms, and a max conductance of 200nS. Now the model cell exhibits a profile similar to the real cell (Figure 3C).

The membrane constant explains the difference between the two cell types

Using the model of the neuron with an AHP conductance, I varied the time constant of the cell; first by changing the capacitance of the model cell (figure 4A), and next by changing the resistance of the model cell (Figure 4B). As the time constant of the cell increases, the dependence of sine amplitude decreases. The model cell with a longer time constant, takes longer to charge, and therefore responds more slowly to changes in inhibitory input.

I then measured the membrane time constant of my recorded cells, by calculating the amount of time it took for a cell to reach 67% of its max voltage when a current pulse was applied to the cell. The average time constant for the cells that gave a profile similar to figure 2A was 18ms, and the average time constant for the cells that gave a profile similar to figure 2B was 38ms. Therefore, it seems likely that the time constant is what contributes to the two different cell profiles.

Figure 3. AHP conductance is important in regulating spike rate.

The number of spikes in a 250ms pulse is plotted against the mean level of inhibition and amplitude of the sine wave for a model cell with no afterhyperpolarization (AHP) conductance (A) and with AHP conductance (C). Voltage trace when just excitatory current is injected into a model cell with no AHP conductance.(B) and into a real cell (D). The model cell with an AHP conductance shows a similar spike-rate dependence on mean level of inhibition and sine amplitude.
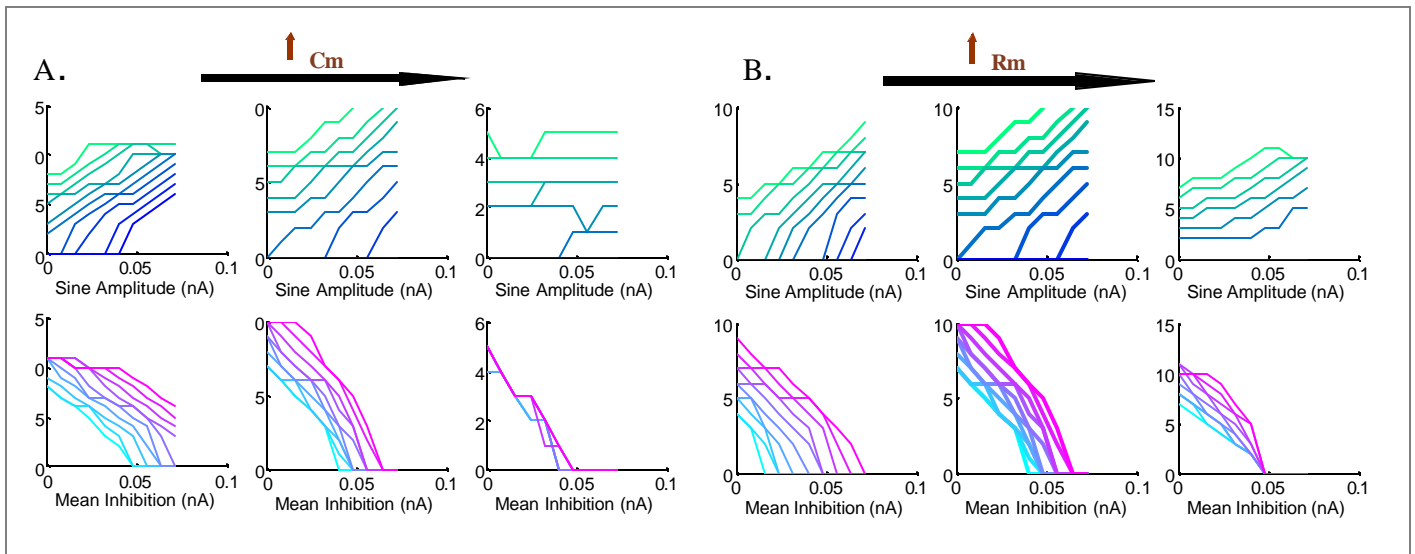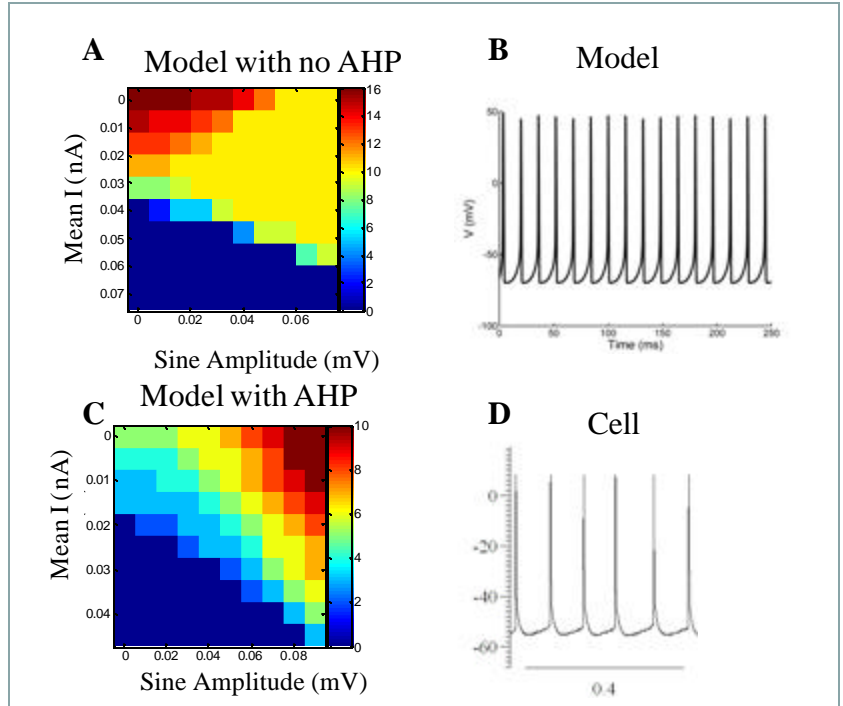

Figure 4. Affects of increasing the membrane time constant on model cell's response to inhibitory input. Changing the time constant of the cell by increasing the cell's capacitance (A) or resistance (B) results in less dependence on sine amplitude (top) and more dependence on the level of mean inhibition (bottom).

Discussion

This paper focused on the effects of synchronized input from inhibitory populations on the spike rate of pyramidal neurons. I found that simulating or modeling increasing in synchronized inhibitory input to a cell increased the spike rate of some pyramidal neurons. This finding may help to explain some curious data from the Reynolds lab. They found that during an attention task the spike rate of both putative fast-spiking inhibitory

neurons, and putative regular spiking pyramidal neurons increased when attention was directed inside the receptive field of a neuron (Mitchell et al., 2007). The results of this project may help explain how it is possible to get a simultaneous increase in inhibition and excitation. Attention is also associated with increases in gamma synchrony, so even though the level of inhibition is increasing, a simultaneous increase in the synchrony of inhibition may lead to increased spiking in the pyramidal neurons.

These results may also help to elucidate the role of different neuronal types in the network. We found that different pyramidal cells behave differently to changes in inhibitory input. Some cells are insensitive to changes in inhibitory synchrony, while other cells increase their firing rate. I found that the time constant of the cells most likely explains this difference. Future studies will focus on the functional consequences of these differences between these two populations of pyramidal neurons. What are the pre-synaptic targets of these cells? What are their post-synaptic targets? How does that activity of these two different neuronal types contribute to flow of cortical information.   These and other questions will involve more sophisticated modeling, as well as genetic and viral techniques being developed in the Callaway lab that can change the ability of inhibitory neurons to synchronize in the intact network.

References

M. Bartos *et al.*, Synaptic mechanisms of synchronized gamma oscillations in inhibitory interneuron networks, *Nat. Rev. Neurosci.* **8** (2007), pp. 45–56.

Erisir A, Lau D, Rudy B, Leonard CS. Function of specific K(+) channels in sustained high-frequency firing of fast-spiking neocortical interneurons. J Neurophysiol. 1999 Nov;82(5):2476-89.

C.M. Gray *et al.*, Oscillatory responses in cat visual cortex exhibit inter-columnar synchronization which reflects global stimulus properties, *Nature* **338** (1989), pp. 334–337

Hasenstaub A, Shu Y, Haider B, Kraushaar U, Duque A, McCormick DA. Inhibitory postsynaptic potentials carry synchronized frequency information in active cortical networks. Neuron. 2005 Aug 4;47(3):423-35.

J.G. Jefferys *et al.*, Neuronal networks for induced '40 Hz' rhythms, *Trends Neurosci.* **19** (1996), pp. 202–208.

Mitchell JF, Sundberg KA, Reynolds JH. Differential attention-dependent response modulation across cell classes in macaque visual area V4. Neuron. 2007 Jul 5;55(1):131-41.

B. Pesaran et al., Temporal structure in neuronal activity during working memory in macaque parietal cortex, Nat. Neurosci. 5 (2002), pp. 805–811.

M.A. Whittington *et al.*, Synchronized oscillations in interneuron networks driven by metabotropic glutamate receptor activation, *Nature* **373** (1995), pp. 612–615.